P1.25 A SYNERGISTIC SURFACE BRDF/ALBEDO RETRIEVAL WITH MODIS AND MISR OBSERVATIONS 1. INTERCOMPARISON

Yufang Jin, Feng Gao, Crystal Schaaf, and Alan Strahler
Department of Geography, Boston University, Boston, Massachusetts

Carol Bruegge, John Martonchik, and David Diner
Jet Propulsion Laboratory, California Institute of Technology, Pasadena, California

1. INTRODUCTION

Surface albedo, the ratio of radiative energy reflected by land surface to incoming radiation, plays a key role in surface energy budget and hence has significant influences on climate. Satellite observations offer a great opportunity for global surface albedo retrieval from space. The acquisition of angular measurements by an individual sensor, however, is limited by its scanning configuration, the platform's orbital characteristics and cloud appearances. Surface Bidirectional Reflectance Distribution Function (BRDF) characterizes the anisotropy of surface reflectance and if specified accurately, can be used to retrieve surface albedo from limited directional observations of satellites (Wanner et al., 1997; Schaaf et al., 2001) .

The MODerate Resolution Imaging Spectro−radiometer (MODIS) and Multi−angle Imaging Spectroradiometer (MISR), on board the same TERRA platform, employ different observation concepts and both provide surface BRDF and albedo products with different retrieval algorithms. This paper intends to analyze the similarities and differences between MODIS and MISR surface bidirectional reflectance (BRF) and albedo products, as the first step in our ongoing effort to combine MODIS and MISR observations for better surface BRDF/albedo retrieval.

2. INSTRUMENT AND DATA

MODIS−TERRA is a cross−track imager and provides a near−daily global coverage. The directional samplings are accumulated through a time series of observations, and global surface BRDF and albedo are produced for each 16−day period. MISR, however, takes the novel approach of imaging the the earth almost simultaneously in nine different view directions (Diner et al., 1998). Its view angles range from 26.2° to 70° both in forward and afterward direction in addition to nadir looking. MISR scans along−track and hence complements MODIS in the azimuth dimension.

Daily atmospheric corrected surface directional reflectances are gridded into one kilometer resolution (Vermote et al., 2001) to serve as the input data for the MODIS BRDF/Albedo product and are used for this study. We reprojected and resampled the MISR level 2 surface products (Martonchik et al., 1998) and geometric parameter data from Space Oblique Macerator (SOM) to Integerized Sinusoidal Grid (ISG). Two ISG tiles acquired in early January and one in February 2001 were selected and four corresponding MISR swaths were extracted to represent different land cover types and sampling geometry (Table 1). Radiometric adjustments were applied to the first three swaths according to recent calibration data (Bruegge et al., 1997). The dominant land cover types are bare desert, semi−desert and shrubs. Figure 1 shows typical sampling geometries of MODIS and MISR over the

Table 1. Study areas represented by MODIS ISG tile number and MISR path/orbit as well as acquiring dates.

Lat., Lon.	Land type	MODIS tile (date)	MISR path, orbit (date)
30°~40°N 104°~130°W	Shrubland	h08, v05 1~16, Jan.	P042, O005569 3, Jan.
10°~20°N 0°~10°E	Desert	h18, v07 1~16, Jan.	P188, O005549 2, Jan.
		h18, v07 1~16, Jan.	P193, O005593 5, Jan.
20°−30°S 0°~10°E	Shrubland	h20, v11 2~17, Feb.	P174, O006218 17, Feb.

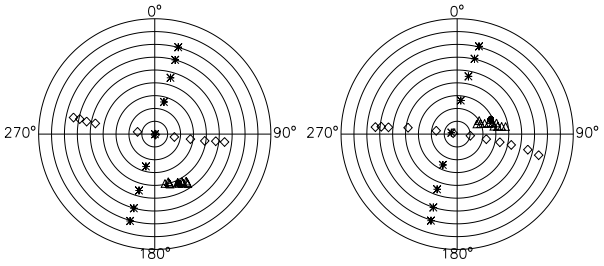

Figure 1. Angular sampling from MODIS and MISR observations in Sahel in early January (left) and in South Africa in early February (right). Radius of circles represents zenith angle with 10° increment (zero zenith angle is in the center) and polar angle represents azimuth (zero azimuth, North, is on the top). Diamond and asterisk: MODIS and MISR viewing direction; Triangle and solid dot: sun locations of MODIS and MISR overpass.

Corresponding author address: Yufang Jin, Boston Univ., Dept. Of Geography, Boston, MA 02215; email: yfj@crsa.bu.edu

Study areas. Both MODIS and MISR observations are between the principal plane (PP) and cross principal plane (CPP) over Sahel and California in early January. MODIS observations are closer to the PP while MISR observations fall between the PP and CPP in South Africa during early February. The change of solar zenith angles of MODIS observations during the 16 day periods are within 10° except for South Africa, where the solar zenith changes about 20°.

3. RESULTS

The anisotropy of surface reflectivity for shrubs on soil (Sahel) and on grass (South Africa) are demonstrated in both MODIS and MISR BRFs (Figure 2). Both MODIS accumulated angular observations and MISR simultaneous observations capture the characteristics of vegetation reflectance, such as the stronger backward scattering and hot spot effect. Surface directional reflectances of MODIS and MISR are very similar in tile h08v05 and h18v07, where both viewing azimuths are between the PP and CPP (Figure 2, top panels). The RossThickLiSparse−Reciprocal (RTLSR) BRDF model (Wanner et al., 1995) inverted with MODIS data predicts very well the shape of surface directional reflectance at MISR view geometry over these regions. However, surface reflectances observed from MODIS show larger angular variations than those from MISR in tile h20v11 (path 174), due to the fact that MODIS observations are closer to the PP in this tile during February (Figure 2, bottom panels). The decrease of predictability in tile h20v11 indicates that MISR observations can add extra angular information to MODIS observations when their sampling geometries are not equivalent.

Direct intercomparison of BRFs can not be made since MODIS and MISR acquire observations at different sampling geometry. Close to nadir, however, there are some possibilities that MODIS and MISR observing angles are similar. We extracted near nadir observations with viewing zenith and solar zenith difference less than 5° and relative azimuth difference less than 10°. The scatter plots of MODIS BRFs versus MISR BRFs at near nadir show a strong linear relationship, especially in red and green band (Figure 3, top panels). Normalized Difference Vegetation Index (NDVI) distribution demonstrates two modes with 0.15 as the break point. Pixels with NDVI higher than 0.15 are mostly from path 174 in South Africa, which is dominated by shrubs with grass underneath, and therefore its histograms of MODIS and MISR near−nadir BRFs were plotted separately from other swaths in Figure 3 (bottom panels). The shapes of histograms are very similar, indicating that both MODIS and MISR capture similar spatial variations of surface nadir reflectances.

In general MODIS BRFs agree very well with MISR in the green band for all pixels and are consistently lower by around 8 percent in the red. The largest difference is in the blue band, where MODIS BRFs are generally higher than MISR, due to the difficulty of aerosol retrieval and atmospheric correction in sparsely vegetated area. Theoretically, the difference between MODIS and MISR aerosol correction should lead to consistent differences between MODIS and MISR surface reflectance in the blue, green and red band. This is shown by the fact that the correlation between relative differences in red and blue is as high as 0.54. However, band center shifts might offset the expected differences. Both MODIS and MISR centers at 0.56 µm in green, and MODIS blue band center is 23 nm larger than MISR while red band center of MODIS is 26 nm less than MISR. We find that MODIS near nadir reflectance is close to MISR in tile h18v07 and h08v05, but is lower than MISR by 14 percent in tile h20v11 (South Africa). Further examination of MISR BRF images shows some distinct blocks in NIR and blue, where larger differences in NIR occur. It is recognized that the MISR algorithms were in updating period. In fact, the images of MISR surface products acquired beginning May 2001 is not spotty. Another possible reason is vegetation growth since MISR path 174 was acquired on February 17, the last day of the MODIS 16 day period in early February.

Another way to compare MODIS and MISR reflectance is to use a BRDF model to infer surface reflectance at geometries beyond observations. We inverted the RTLSR BRDF model with extracted MISR BRFs. The derived parameters were used to predict surface reflectance at the sampling geometry of MODIS at the same day. The scatter plots and histograms of MODIS BRFs against MISR concurrent predictions show similar results as those of near−nadir observations. The difference, however, increases for path 174 due to the same reasons discussed above.

Table 2. Correlation and differences (mean and standard deviation) between MODIS black sky albedo at MISR−overpass solar zenith angle and MISR directional hemispherical reflectance in tile h18v07.

Band	R	Difference	Relative Difference
NIR	0.88	−0.046 (0.068)	−7.3% (9.6%)
Red	0.96	−0.047 (0.033)	−10.0% (6.6%)
Green	0.96	−0.019 (0.020)	−6.2% (6.4%)
Blue	0.82	0.024 (0.017)	20.0% (15.3%)

The operational MODIS black sky albedo (BSA) is produced at local solar noon, while MISR directional hemispherical reflectance (DHR) is the direct beam albedo during the MISR overpass. We here therefore derived MODIS BSA at MISR−overpass solar zenith angle off−line instead of using MODIS operational BSA product. The similarity and difference of MISR DHR and MODIS black sky albedo again follow the pattern of near nadir reflectance although the magnitude of differences increases (Table 2). MISR DHR is derived

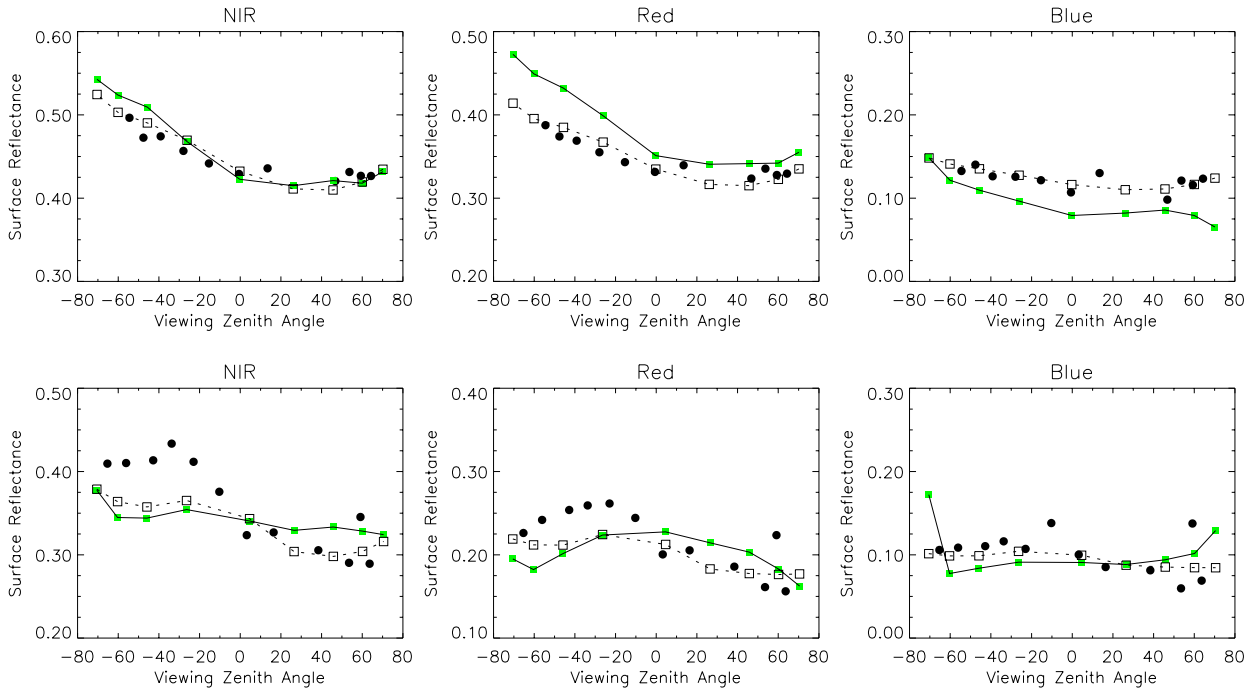

Figure 2. Surface directional reflectances observed from MODIS (dark solid dot) and MISR (light solid square, solid line) and predicted surface reflectance at MISR sampling geometry from MODIS observations (open square, dashed line). Top panel represents sparse shrubs on bare soil in Sahel, and bottom panel represents the shrubs on grass in South Africa.

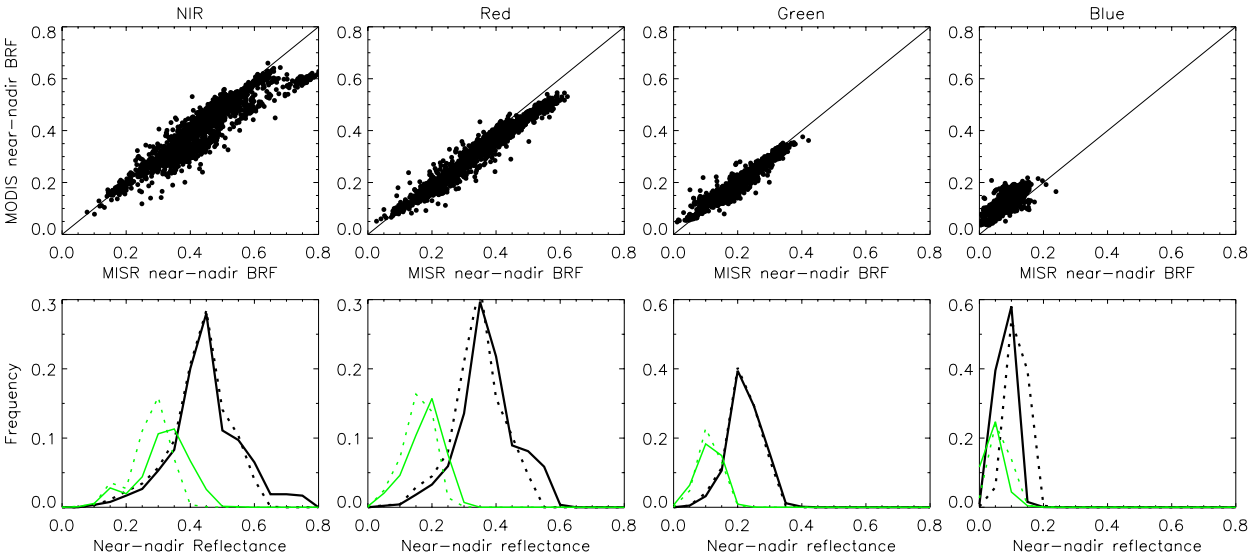

Figure 3. Scatter plots (top panels) and histograms (bottom panels) of MODIS versus MISR near nadir surface reflectances. Dashed line represents distributions of MODIS reflectances and solid line MISR reflectances. Light color is for tile h20v11 in South Africa (path 174) and dark color for other two tiles.

from retrieved surface hemispherical directional reflectances using a parameterized BRDF model (MRPV) (Engelsen et al., 1996), while MODIS albedo is based on RTLSR model. In order to examine the possible error induced by BRDF models, we generated surface albedo from MISR BRFs using MODIS algorithm and compared it with MISR DHR. The difference is within 3 percent, indicating that RTLSR and modified RPV model are similar in their ability to invert surface BRDF and to retrieve surface albedo as

previously demonstrated by Lucht (1998), Gao (2000), and Bicheron (2000).

4. CONCLUSIONS

We explored three intercomparisons between MODIS and MISR products with an aim of combining MODIS and MISR data to improve the retrieval of BRDF and albedo: near−nadir surface reflectance, surface reflectance at MODIS viewing geometry predicted by inversion of same day MISR observations, and MODIS black sky albedo under MISR−overpass solar zenith angle versus MISR directional hemispherical reflectance. Results show that

a) MODIS and MISR near−nadir BRF/DHR are very similar in the green band and MODIS BRF/DHR are generally 8 percent lower than MISR in the red band. MODIS BRF/DHR are around 20 percent higher than MISR in the blue band. Special attention should be paid to the NIR band, where differences may be dependent on vegetation status.

b) Largest relative differences appear in the blue band and the correlation between relative differences in the red band and blue band are as high as 0.54, indicating that these differences are probably due to the atmospheric correction differences.

c) Opposite band center shift seems to explain the opposite biases in blue and red of MODIS BRF/DHR relative to those of MISR. However, more studies about spectral differences need to be done in the future.

d) Information content of MODIS and MISR angular observations is very similar when observations of them are made between principal plane and cross principal plane. However, additional angular information can be added to other if they do not have equivalent angular samplings.

It should be noted that MODIS has started reprocessing a consistent one year product and that the MISR level 2 algorithms were being updated at the time of the intercomparison presented here. In the future, the most current data will be analyzed for various land cover types, sampling geometries and atmospheric conditions. TOA (top−of−atmosphere) radiance comparisons can be used to further determine if biases are caused by calibration or atmospheric correction.

REFERENCES

Diner, D. J., J. C. Beckert, T. H. Reilly, C. J. Bruegge, J. E. Conel, R. Kahn, J. V. Mortonchik, T. P. Ackerman, R. Davies, S. A. W. Gerstl, H. R. Gordon, J.−P. Muller, R. B. Myneni, P. J. Sellers, B. Pinty, and M. M. Verstraete, 1998: Multi−angle Imaging Spectro−Radiometer (MISR) instrument description and experiment overview, *IEEE Trans. Geosci. Remote Sens.*, 36, 1,072−1,085

Bicheron, P., and M. Leroy, 2000: Bidirectional Reflectance Distribution Function signatures of major biomes observed from space, *J. Geophys. Res.*, 105, 26,669−26,681

Bruegge, C. J., N. L. Chrien, R. Ando, and B. Chafin, 1997: In−flight radiometric calibration of the EOS/ MISR multicamera instrument. *Earth Observing System*, *Proc. SPIE 3117*, San Diego, CA, 28−29 July 1997

Engelsen, O., B. Pinty, M. M. Verstraete, and J. V. Martonchik, 1996:, Parametric bidirectional reflecance factor models: evaluations, improvements and applications, *Rep. EU 16426*, 114, Joint. Res. Cent. Eur. Comm., Ispra, Italy, 1996

Gao, F., X. Li, A. Strahler, and C. Schaaf, 2000: Evaluation of the LiTransit Kernel for BRDF modeling, *Remote Sens. Rev.*, 19, 205−224

Martonchik, J. M., D. J. Diner, R. A. Kahn, T. P. Ackerman, M. M. Verstraete, B. Pinty,H. R. Gordon, 1998: Techniques for the retrieval of aerosol properties over land ocean using multiangle imaging, *IEEE Trans. Geosci. Remote Sens.*, 36, 1,212−1,227

Schaaf, C. B., F. Gao, A. H. Strahler, W. Lucht, X. Li, T. Tsang, N. C. Strugnell, X. Zhang, Y. Jin, J.−P. Muller, P. Lewis, M. Barnsley, P. Hobson, M. Disney, G. Roberts, M. Dunderdale, C. Doll, R. d'Entremont, B. Hu, S. Liang, and J. L. Privette, 2001: First Operational BRDF, Albedo and Nadir Reflectance Products from MODIS, submitted to *Remote Sens. Environ.*

Wanner, W., A. H. Strahler, B. Hu, P. Lewis, J.−P. Muller, X. Li, C. B. Schaaf, and M. J. Barnsley**,** 1997: Global retrieval of bidirectional reflectance and albedo over land from EOS MODIS and MISR data: theory and algorithm, *J. Geophys. Res.*, 102, 17,143−17,162

Wanner, W., X. Li, and A.H. Strahler, 1995: On the derivation of kernels for kernel−driven models of bidirectional reflectance, *J. Geophys. Res.*, 100, 21,077−21,089

Lucht, W., 1998: Expected retrieval accuracies of bidirectional reflectance and albedo from EOS−MODIS and MISR angular sampling, *J. Geophys. Res.*, 103, 8,763−8,778

Vermote, E. F., N. Z. Saleous, and C. O. Justice, 2001: Atmospheric correction of MODIS data in the visible to middle infrared: First results, submitted to *Remote Sens. Environ.*